

MAKING THE URBAN SKY VIEW FACTOR WITH NUMERICAL MODELS CONSISTENT WITH RADIATION HEAT TRANSFER THEORY

“Technical Brief”

N. U. Rehman^{1,2*}, T. N. Anderson¹ and R. J. Nates¹

¹Department of Mechanical Engineering, Auckland University of Technology, Auckland, New Zealand

²School of Engineering Trades and Technology, Southern Institute of Technology, Invercargill 9840, New Zealand.

*Corresponding author:

Tel: +64 39482772

Email address: naveed.urrehman@sit.ac.nz

Abstract

This work proposes a method for removing the inconsistency between the numerical models used for determining the sky view factor (*SVF*) in an urban environment and fundamental radiation heat transfer theory. For this purpose, a transformation of the coordinate system from global to surface was developed, which corrected the measurement of the angular coordinates of the elements in the discretized sky vault. The transformation was deployed in a published numerical model and was validated in a non-urban environment with a widely used analytical expression for the *SVF*, with which it was found to be in excellent agreement. The method was subsequently applied to an urban scenario and the results were compared with the original numerical model. The proposed method provides a better determination of the *SVF* as a function of the surface azimuth and tilt angle.

Keywords: sky view factor; sky vault; sky element

1. Introduction

The diffuse solar irradiance (D , W/m^2) reaching a receiving surface can be obtained by multiplying the diffuse irradiance on the horizontal (D_o , W/m^2) by a mathematical ratio, called the sky view factor (SVF), as shown in Eq. (1).

$$D = D_o \cdot SVF \tag{1}$$

The magnitude of D_o can be obtained from historical measurements or by using models [1-4], while the value of SVF is determined analytically or numerically [5,6]. To analytically calculate the SVF for a non-urban site, the most widely used expression is that of Liu and Jordan (SVF_{LJ}) [7] which features prominently in the literature [8-12] and for which an analytical proof has been developed [13]. However, in an urban context, Liu and Jordan's relationship is inadequate for describing the true sky view factor. In an attempt to address this, Li and Lam [14] suggested a numerical method for estimating the SVF of urban sites, based on computing the sum of incoming radiances.

In this respect, Tregenza and Sharples [15] had previously demonstrated a similar approach in which the sky vault was divided into elements, and the individual radiances approaching from each element were analyzed. The method considered both the dilation and cosine effect associated with the solid angles representing these elements. The dilation factor accounted for the expansion of solid angles, from the zenith to the base of the sky vault, while the cosine effect accounted for the incidence angle between the direction of radiance and the normal to the surface.

Following this type of approach, Siraki and Pillay [16] devised a technique based on disintegrating the sky vault to determine the SVF of urban sites. In implementing this, the method they used in analyzing individual radiances was similar to that proposed by Li and Lam [14]; however, their approach to the disintegration of the vault was different, and did not account for the dilation and cosine effect. Siraki and Pillay found that for a non-urban site, their simulation results were similar to those arrived at analytically, vis-à-vis SVF_{LJ} .

Building on this work, Tripathy et al. [17] used the same model and proposed a nomograph for determining the SVF in a pseudo-urban environment consisting of infinite-length buildings of constant height around the surface. Rehman and Siddiqui [18] improved the model by accounting for the dilation and cosine effects.

In considering these approaches, however, it is important to note that these models use a fixed horizontal plane for determining the angular coordinates of elements when calculating the dilation factor. Badescu [19] and Rakovec and Zaksek [20] suggested that such an approach was inconsistent with the fundamental concepts of radiation heat transfer and proposed analytical relationships that were suitable for non-urban sites only. However, these relationships were found to be mathematically incorrect, as proved in [21]. Removing the errors led to the same relationship as was proposed by Liu and Jordan [7]. However, to the authors' knowledge, there has been no correct numerical model developed that can successfully analyze urban sites. Therefore, this work presents a numerical method based on a revision of Rehman and Siddiqui's [18] model (hereafter termed RS-model) that has been made fully consistent with the theory of radiation heat transfer.

2. Background

In the vault disintegration technique, the elements are small areas on the surface of a vault of unit radius (Fig. 1(a)). The area of an element is therefore equal to the magnitude of the solid angle it subtends at the center of the vault, and is mathematically expressed by Eq. (2):

$$d\omega = d\alpha dy \cos \alpha \tag{2}$$

where $d\omega$ (sr) is the solid angle, $d\alpha$ is the altitudinal height of the element, dy is the longitudinal width of the element located at the base plane of the vault and α is the altitude angle of the element.

For a constant value of $d\alpha$ and dy , for all elements, the magnitude of the solid angle of any element only depends upon $\cos \alpha$. Therefore, any inappropriate measurement of α may induce errors in the calculation of the SVF . Although Eq. (2) was used in the RS-model, the reference for measuring α was assumed fixed at the horizontal, irrespective of the surface tilt angle (Fig. 1(b)), which, from the perspective of radiation heat transfer, is inappropriate. According to radiation heat transfer theory the reference plane for measuring α should be the receiving surface [22-24].

Changing the reference plane in the published models alters the angular coordinates of the elements associated with the sky and the projection of urban features onto the vault. In these models, the coordinates were measured relative to a global coordinate system (GCS) in

which the altitude (α_g) and azimuth (γ_g) angles were measured from the horizontal and from some standard cardinal direction, e.g. true south, respectively. However, considering a surface-aligned coordinate system (SCS), the altitude (α_s) and azimuth (γ_s) angles need to be measured from the surface and from the line of orientation of the surface respectively, as shown in Fig. 1(b and c). The method for transforming the coordinates of elements from GCS to SCS is explained in the next section.

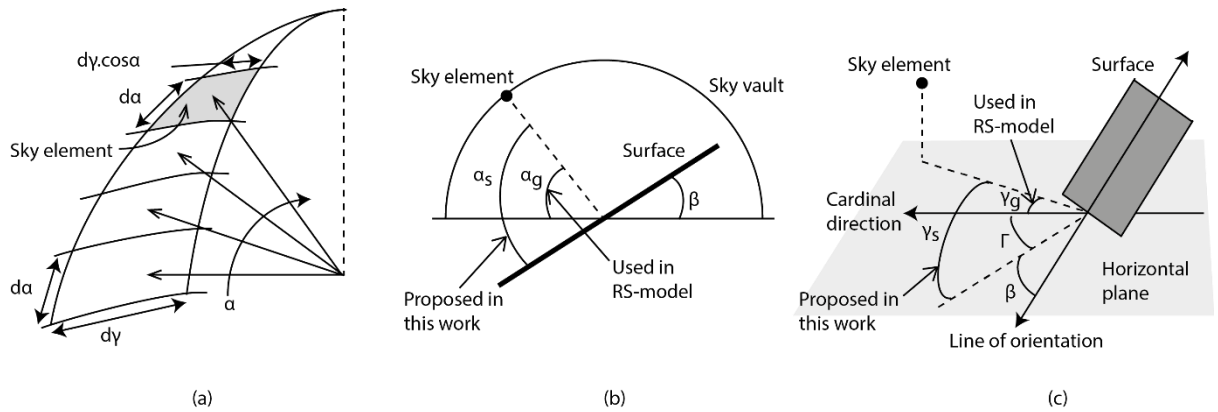


Fig. 1: (a) Area of an element in a disintegrated sky vault; (b) Definition of altitudinal coordinates of elements used in published models and in this work; (c) Definition of azimuthal coordinates of elements used in published models and in this work

3. Method

The method follows the same approach as that described in the previously published models ([14-18]), except that the coordinates of elements are transformed from a GCS to an SCS, with a receiving point on the surface as the origin (Fig. 2).

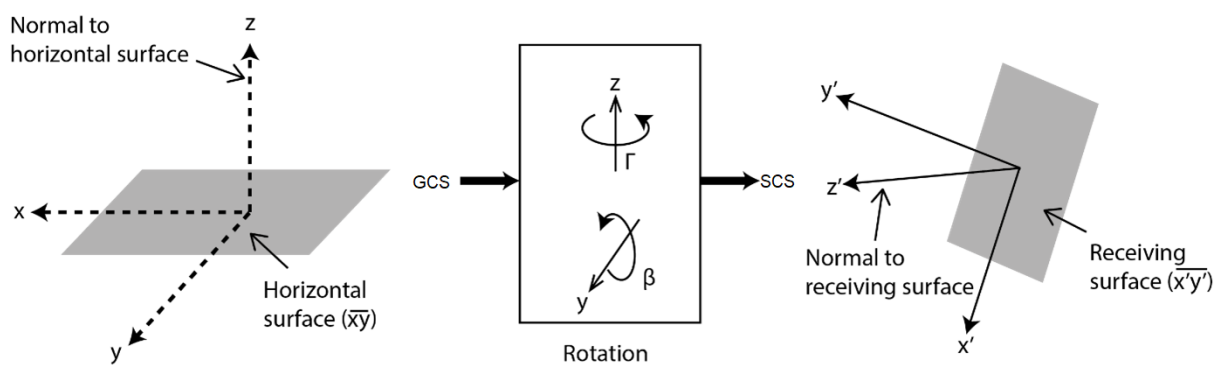


Fig. 2: Global coordinate system (GCS) rotated to form a surface coordinate system (SCS)

For the transformations, the Cartesian axis in the GCS is expressed in terms of x , y and z where a plane \overline{xy} forms a horizontal surface, z is aligned with the geographical zenith

passing through the point on the surface and \hat{i} , \hat{j} and \hat{k} are unit vectors along x , y and z . Similarly, the Cartesian axis in the SCS is expressed as x' , y' and z' where the plane $\overline{x'y'}$ forms the receiving surface, z' is aligned normal to the surface and \hat{u} , \hat{v} and \hat{w} are the unit vectors along x' , y' and z' , respectively. Hence, in moving between the coordinate systems the GCS should be rotated about the z -axis and y -axis as shown in Eq. (3) and Eq. (4):

$$[\hat{u} \ \hat{v} \ \hat{w}]^T = R[\hat{i} \ \hat{j} \ \hat{k}]^T \quad (3)$$

where Γ and β are the surface azimuth and tilt angles respectively, T is matrix transpose and R is the rotation matrix:

$$R = \begin{bmatrix} \cos \Gamma & -\sin \Gamma & 0 \\ \sin \Gamma & \cos \Gamma & 0 \\ 0 & 0 & 1 \end{bmatrix} \begin{bmatrix} \cos(-\beta) & 0 & \sin(-\beta) \\ 0 & 1 & 0 \\ -\sin(-\beta) & 0 & \cos(-\beta) \end{bmatrix} \quad (4)$$

Hence, considering an element located at (γ_g, α_g) in a GCS, the vector pointing to this element would be as determined by Eq. (5):

$$\hat{G} = [\cos \gamma_g \cos \alpha_g \quad \sin \gamma_g \cos \alpha_g \quad \sin \alpha_g] \quad (5)$$

Alternatively, using Eq. (3), the vector pointing to the same element in the SCS would be given by Eq. (6) (see ‘‘Appendix 1’’ for a numerical example):

$$\hat{S} = R \hat{G}^T \quad (6)$$

The final required coordinates of this element in a SCS would be (γ_s, α_s) , such that the conditions outlined in Eq. (7) and Eq. (8) are upheld.

$$\gamma_s = \begin{cases} 0^\circ & , \text{proj}_{\overline{x'y'}}(\hat{S}) = [0 \ 0 \ 0], R(3) = -1 \\ 180^\circ & , \text{proj}_{\overline{x'y'}}(\hat{S}) = [0 \ 0 \ 0], R(3) \neq -1 \\ \phi_{\text{proj}_{\overline{x'y'}}(\hat{S}), \hat{u}} & , \text{proj}_{\overline{x'y'}}(\hat{S}) \neq [0 \ 0 \ 0], \phi_{\text{proj}_{\overline{x'y'}}(\hat{S}), \hat{v}} \leq 90^\circ \\ 360^\circ - \phi_{\text{proj}_{\overline{x'y'}}(\hat{S}), \hat{u}} & , \text{proj}_{\overline{x'y'}}(\hat{S}) \neq [0 \ 0 \ 0], \phi_{\text{proj}_{\overline{x'y'}}(\hat{S}), \hat{v}} > 90^\circ \end{cases} \quad (7)$$

and

$$\alpha_s = \begin{cases} 90^\circ & , \text{proj}_{\overline{x'y'}}(\hat{S}) = 0 \\ \phi_{\text{proj}_{\overline{x'y'}}(\hat{S}), \hat{s}} & , \text{proj}_{\overline{x'y'}}(\hat{S}) \neq [0 \ 0 \ 0], \phi_{\hat{w}, \hat{s}} \leq 90^\circ \\ -\phi_{\text{proj}_{\overline{x'y'}}(\hat{S}), \hat{s}} & , \text{proj}_{\overline{x'y'}}(\hat{S}) \neq [0 \ 0 \ 0], \phi_{\hat{w}, \hat{s}} > 90^\circ \end{cases} \quad (8)$$

where the functions ϕ and $proj$ are as defined in the “Appendix 2”.

4. Results and discussion

Using the method discussed in the previous section in the RS-model, for a non-urban site, showed excellent agreement with the SVF_{LJ} as shown in Fig. 3. Extending on this, the simulations were also performed for the urban site shown in Fig. 4, as used by Siraki and Pillay [16] and Rehman and Siddiqui [18].

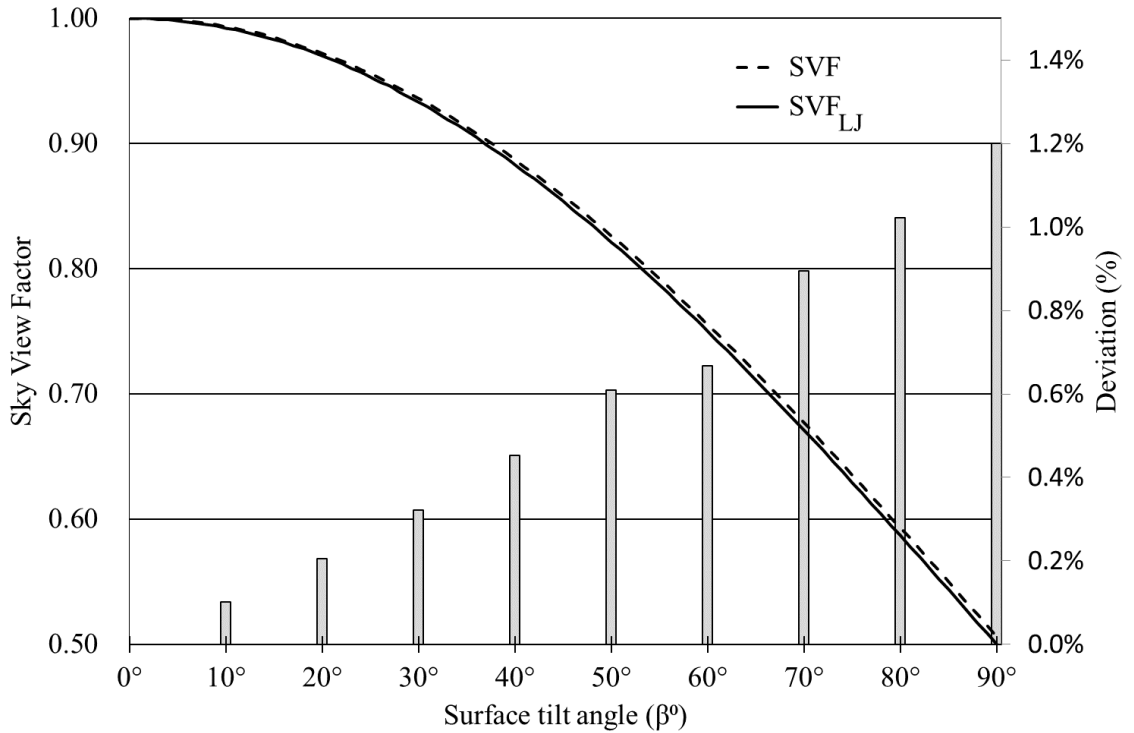


Fig. 3: Comparison of SVF_{LJ} and the proposed method (simulations performed for a non-urban site, $d\alpha = d\gamma = 0.1^\circ$)

Fig. 5 illustrates the difference between the predictions from the original RS-model and this model. It can be seen that the projection of the urban features on the vault is fixed in the RS-model (Fig. 5a and b) irrespective of the receiving surface tilt angle, whereas in the revised model (Fig. 5c and d), the projection of an obstacle is patched uniquely for every tilt angle. In this respect, for receiver tilt angles of 30° (Fig. 5a and c) and 60° (Fig. 5b and d), the RS-model was found to underestimate the SVF by 0.82% and 2.97%, respectively.

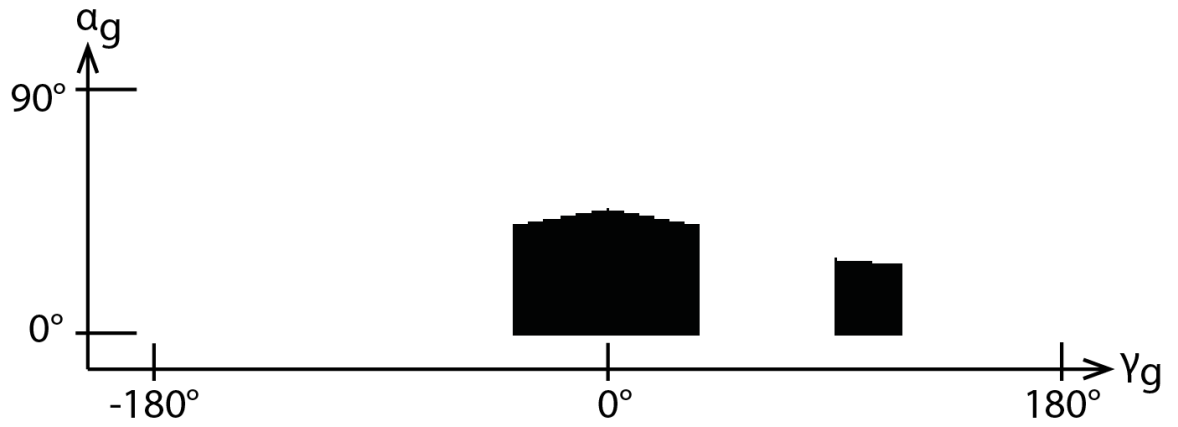


Fig. 4: Projection of the urban scene used in this work on a global coordinate system

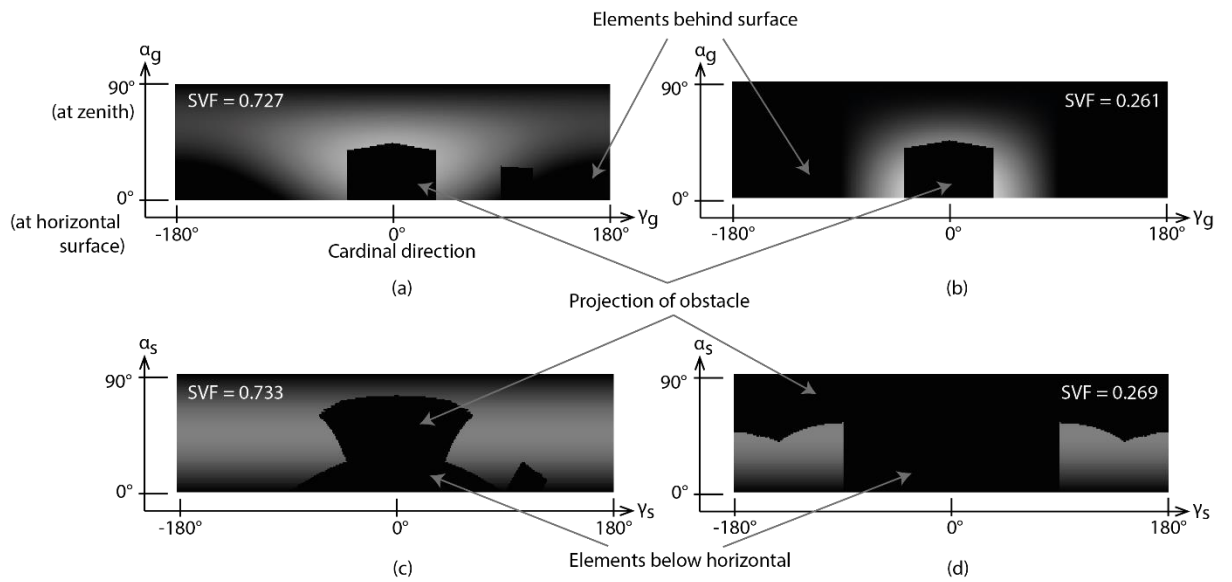


Fig. 5: Sky view factor at an urban site with the surface facing $\Gamma = 0^\circ$, (a) using RS-model at $\beta = 30^\circ$, (b) using RS-model at $\beta = 90^\circ$, (c) using this model at $\beta = 30^\circ$ and (d) using this model at $\beta = 90^\circ$

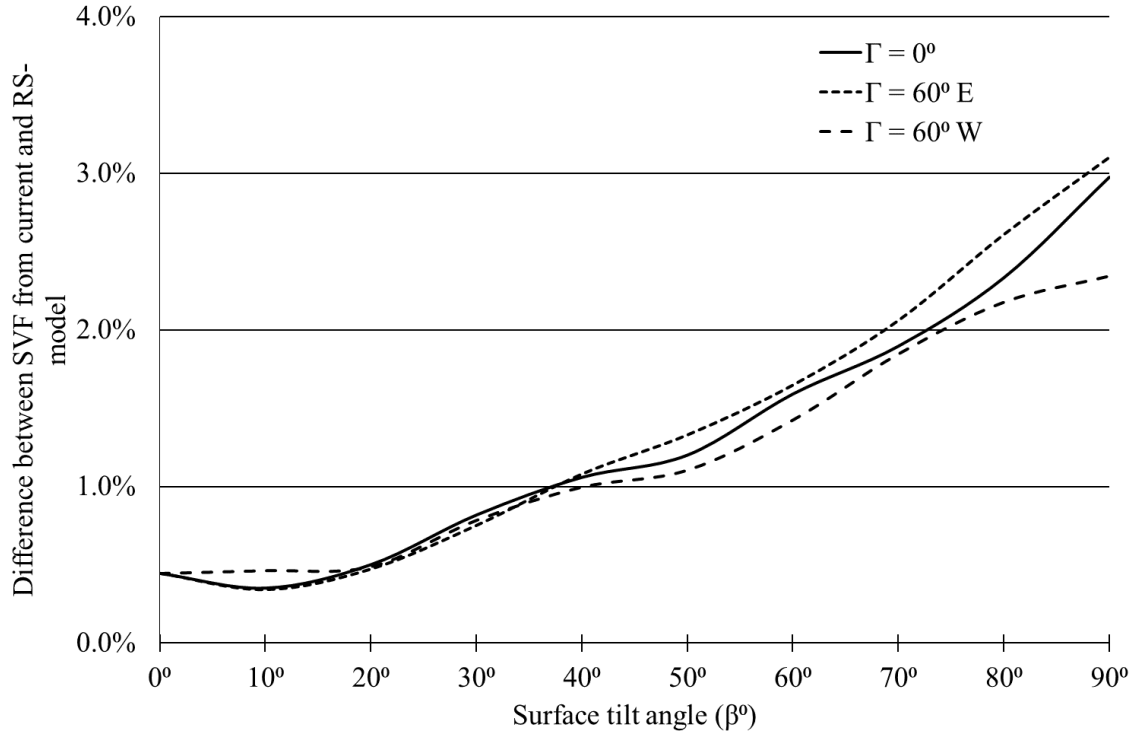


Fig. 6: Difference in SVF between this model and the RS model (simulations performed for the chosen urban site, $d\alpha = d\gamma = 0.1^\circ$)

Hence, for an urban site, the value of SVF obtained by this model shows a noticeable difference from the previous models, the magnitude of which depends upon both the azimuth and tilt angles of the receiving surface as shown in Fig. 6. Reflecting on this point it can be seen that the maximum variation occurs as the receiving surface approaches the vertical ($\beta = 90^\circ$), which could lead to inaccurate assessments of façade performance and underpins the need to maintain consistency with radiation theory.

5. Conclusion

This work demonstrated a method for removing inconsistency with the fundamental theory of radiation heat transfer in models used for determining SVF in an urban environment. As a case study, the method was deployed within an existing model to make it fully consistent with the theory of radiation heat transfer. Simulation results in a non-urban environment were found to be in excellent agreement with Liu and Jordan's model and for an urban site, it was shown that the method provides a better determination of the SVF as a function of the surface azimuth and tilt angle.

Appendix 1

A numerical example for calculating the rotation matrix (R , as in Eq. 4), location of element in GCS (\hat{G} , as in Eq. 5) and the location of element in SCS (\hat{S} , as in Eq. 6) are given in this section.

Let's assume that the surface normal has the azimuth angle and tilt angle given by $\Gamma = 45^\circ$ and $\beta = 45^\circ$, respectively. Then, Eq. 4 can be evaluated as:

$$R = \begin{bmatrix} \cos 45^\circ & -\sin 45^\circ & 0 \\ \sin 45^\circ & \cos 45^\circ & 0 \\ 0 & 0 & 1 \end{bmatrix} \begin{bmatrix} \cos(-\beta) & 0 & \sin(-\beta) \\ 0 & 1 & 0 \\ -\sin(-\beta) & 0 & \cos(-\beta) \end{bmatrix} = \begin{bmatrix} 0.5 & -0.707 & -0.5 \\ 0.5 & 0.707 & -0.5 \\ 0.707 & 0 & 0.707 \end{bmatrix}$$

Also, consider that the element is located in GCS at the altitude and azimuth angle given by $\alpha_g = 45^\circ$ and $\gamma_g = 45^\circ$, respectively. Then, Eq. 5 can be evaluated as:

$$\hat{G} = [\cos 45^\circ \cos 45^\circ \quad \sin 45^\circ \cos 45^\circ \quad \sin 45^\circ] = [0.5 \quad 0.5 \quad 0.707]$$

And so, the location of element in SCS can be obtained by using Eq. 6:

$$\hat{S} = \begin{bmatrix} 0.5 & -0.707 & -0.5 \\ 0.5 & 0.707 & -0.5 \\ 0.707 & 0 & 0.707 \end{bmatrix} \begin{bmatrix} 0.5 \\ 0.5 \\ 0.707 \end{bmatrix} = \begin{bmatrix} -0.457 \\ 0.25 \\ 0.8533 \end{bmatrix}$$

Appendix 2

“ $\phi_{a,b}$ ” is the function describing the angle between two vectors “ a ” and “ b ”, written as:

$$\phi_{a,b} = \cos^{-1} \left(\frac{a \cdot b}{|a||b|} \right)$$

“ $proj$ ” is the function describing the projection of vector “ c ”, written in its parenthesis, over the plane “ \overline{ab} ”, written as:

$$proj_{\overline{ab}}(c) = c - \left(\frac{c \cdot \perp_{\overline{ab}}}{|\perp_{\overline{ab}}|^2} \right) \cdot \perp_{\overline{ab}}$$

where “ \perp ” represents the vector normal to the plane “ \overline{ab} ”, for example, if “ n ” is normal to “ \overline{ab} ” then:

$$\perp_{\overline{ab}} = n$$

Nomenclature

Latin symbols

D	Diffuse solar irradiance reaching a surface (W/m^2)
D_o	Diffuse solar irradiance on the horizontal (W/m^2)
GCS	Global Coordinate System
\hat{G}	Vector pointing to the element in global coordinate system
$\hat{i}, \hat{j}, \hat{k}$	Unit vectors along x, y, z .
R	Rotation matrix
SCS	Surface Coordinate System
SVF	Sky view factor
\hat{S}	Vector pointing to the element in surface coordinate system
$\hat{u}, \hat{v}, \hat{w}$	Unit vectors along x', y', z' .
x, y, z	Cartesian axis in global coordinate system
x', y', z'	Cartesian axis in surface coordinate system

Greek symbols

$d\alpha$	Altitudinal height of the element (degrees)
$d\gamma$	Azimuthal height of the element (degrees)
$d\omega$	Solid angle (sr)
α	Altitude coordinate of the element (degrees)
β	Tilt angle of surface (degrees)
γ	Azimuth coordinate of the element (degrees)
Γ	Surface azimuth angle (degrees)

Subscripts

g	Measured in global coordinate system
LJ	Proposed by Liu and Jordan [7]
s	Measured in surface coordinate system

References

- [1] Maxwell, E. L., Marion, W. F., Myers, D. R., Rymes, M. D., & Wilcox, S. M., 1995. "National Solar Radiation Data Base (1961-1990) - Volume 2," *Final Technical Report National Renewable Energy Lab*.
- [2] Bamisile, O., Oluwasanmi, A., Ejiyi, C., Yimen, Y., Obiora, S., and Huang, Q., 2021, "Comparison of machine learning and deep learning algorithms for hourly global/diffuse solar radiation predictions," *International Journal of Energy Research* . <https://doi.org/10.1002/er.6529>
- [3] Badescu, V., Gueymard, C. A., Cheval, S., Oprea, C., Baci, M., Dumitrescu, A., Iacobescu, F., Milos, I., and Rada, C., 2012, "Computing global and diffuse solar hourly irradiation on clear sky. Review and testing of 54 models," *Renewable and Sustainable Energy Reviews*, 16(3), pp.1636-1656.
<https://doi.org/10.1016/j.rser.2011.12.010>
- [4] Löf, G. O., Duffie, J. A., and Smith, C. O., 1966, "World distribution of solar radiation," *Solar Energy*, 10(1), pp. 27-37. [https://doi.org/10.1016/0038-092X\(66\)90069-7](https://doi.org/10.1016/0038-092X(66)90069-7)
- [5] Massalha, Y., and Appelbaum, J., 2020, "Experimental Verification of the Sky View Factor Model in Multiple-Row Photovoltaic Fields," *Journal of Solar Energy Engineering*, 142(2), 021004. <https://doi.org/10.1115/1.4044979>
- [6] Fathi, N., and Samer, A., 2016, "View factors of flat solar collectors array in flat, inclined, and step-like solar fields," *Journal of Solar Energy Engineering*, 138(6), 061005. <https://doi.org/10.1115/1.4034549>
- [7] Liu, B., and Jordan, R., 1961, "Daily insolation on surfaces tilted towards equator," *ASHRAE Transactions*, 67 (Part 2), pp. 526–541.
- [8] Robinson, N., 1966, *Solar Radiation*, Elsevier, Amsterdam, The Netherlands. OCLC 594335623
- [9] Paltridge, G. W., and Platt, C. M., 1976, *Radiative processes in meteorology and*

climatology, Elsevier, Amsterdam, The Netherlands. ISBN: 0444414444

- [10] Duffie, J. A., and Beckman, W. A., 2013, *Solar engineering of thermal processes*, 3rd ed., Wiley, New York, NY. ISBN 978-0-470-87366-3
- [11] Kalogirou, S. A., 2014, *Solar energy engineering - processes and systems*, 2nd ed., Elsevier, Oxford, UK. ISBN: 9780123972705
- [12] Muneer, T., 2004, *Solar radiation and daylight models*, 2nd ed., Elsevier, New York, NY. ISBN: 978-0-7506-5974-1
- [13] Rehman, N. U., and Uzair, M., 2017, "The proper interpretation of analytical sky view factors for isotropic diffuse solar irradiance on tilted planes," *Journal of Renewable and Sustainable Energy*, 9(5), p. 053702. <https://doi.org/10.1063/1.4993069>
- [14] Li, D. H., and Lam, T. N., 2007, "Determining the optimum tilt angle and orientation for solar energy collection based on measured solar radiance data.," *International Journal of Photoenergy*, Article ID 085401. <https://doi.org/10.1155/2007/85402>
- [15] Tregenza, P.R., and Sharples, S., 1995, "New Daylight Algorithm," University of Sheffield, Sheffield, UK.
- [16] Gharakhani Siraki, A., and Pillay, P., 2012, "Study of optimum tilt angles for solar panels in different latitudes for urban applications," *Solar Energy*, (86) 6, pp. 1920-1928. <https://doi.org/10.1016/j.solener.2012.02.030>
- [17] Tripathy, M., Yadav, S., Sadhu, P. K., and Panda, S. K., 2017, "Determination of optimum tilt angle and accurate insolation of BIPV panel influenced by adverse effect of shadow," *Renewable Energy*, 104, pp. 211-223. <https://doi.org/10.1016/j.renene.2016.12.034>
- [18] Rehman, N. U., and Siddiqui, M. A., 2015, "A novel method for determining sky view factor for isotropic diffuse radiations for a collector in obstacles-free or urban

- sites," *Journal of Renewable and Sustainable Energy*, 7(3), p. 033110. <https://doi.org/10.1016/j.enbuild.2016.07.050>
- [19] Badescu, V., 2002, "3D isotropic approximation for solar diffuse irradiance on tilted surfaces," *Renewable Energy*, 26(2), pp. 221-233. [https://doi.org/10.1016/S0960-1481\(01\)00123-9](https://doi.org/10.1016/S0960-1481(01)00123-9)
- [20] Rakovec, J., and Zaksek, K., 2012, "On the proper analytical expression for the sky-view factor and the diffuse irradiation of a slope for an isotropic sky," *Renewable Energy*, 37(1), pp. 440-444. <https://doi.org/10.1016/j.renene.2011.06.042>
- [21] Xie, Y., Sengupta, M., and Dooraghi, M., 2018, "Assessment of uncertainty in the numerical simulation of solar irradiance over inclined PV panels: New algorithms using measurements and modeling tools," *Solar Energy*, 165.. <https://doi.org/10.1016/j.solener.2018.02.073>
- [22] Cengel, Y. A., 2002. *Heat Transfer: A Practical Approach*, McGraw-Hill Higher Education, New York, USA. ISBN: 9780072458930
- [23] Bergman, T. L., and Incropera, F. P., 2011, *Introduction to heat transfer*, 6th ed., John Wiley and Sons, Hoboken, NJ. ASIN: B00APYBOB0
- [24] Howell, J. R., Menguc, M. P., and Siegel, R., 2015, *Thermal radiation heat transfer*, 6th ed., CRC Press, Boca Raton, FL. ISBN: 9780429190599